AD-A133 082 ICE FORCES ON MODEL BRIDGE PIERS(U) COLD REGIONS RESEARCH AND ENGINEERING LAB HANOVER NH F D HAYNES ET AL. JUL 83 CRREL-83-19 1/1

UNCLASSIFIED F/G 13/13 NL

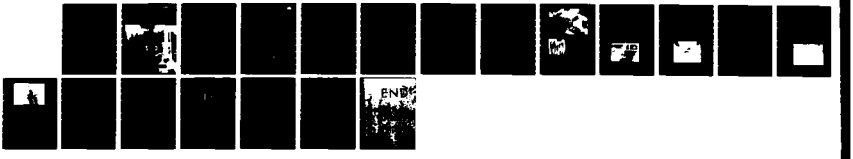

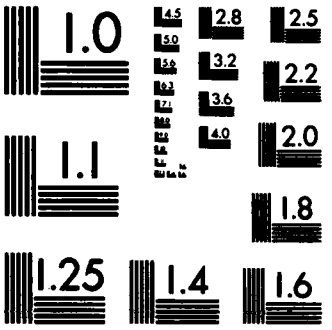

MICROCOPY RESOLUTION TEST CHART
NATIONAL BUREAU OF STANDARDS-1963-A

CRREL REPORT 83-19

US Army Corps of Engineers
Cold Regions Research & Engineering Laboratory

Ice forces on model bridge piers

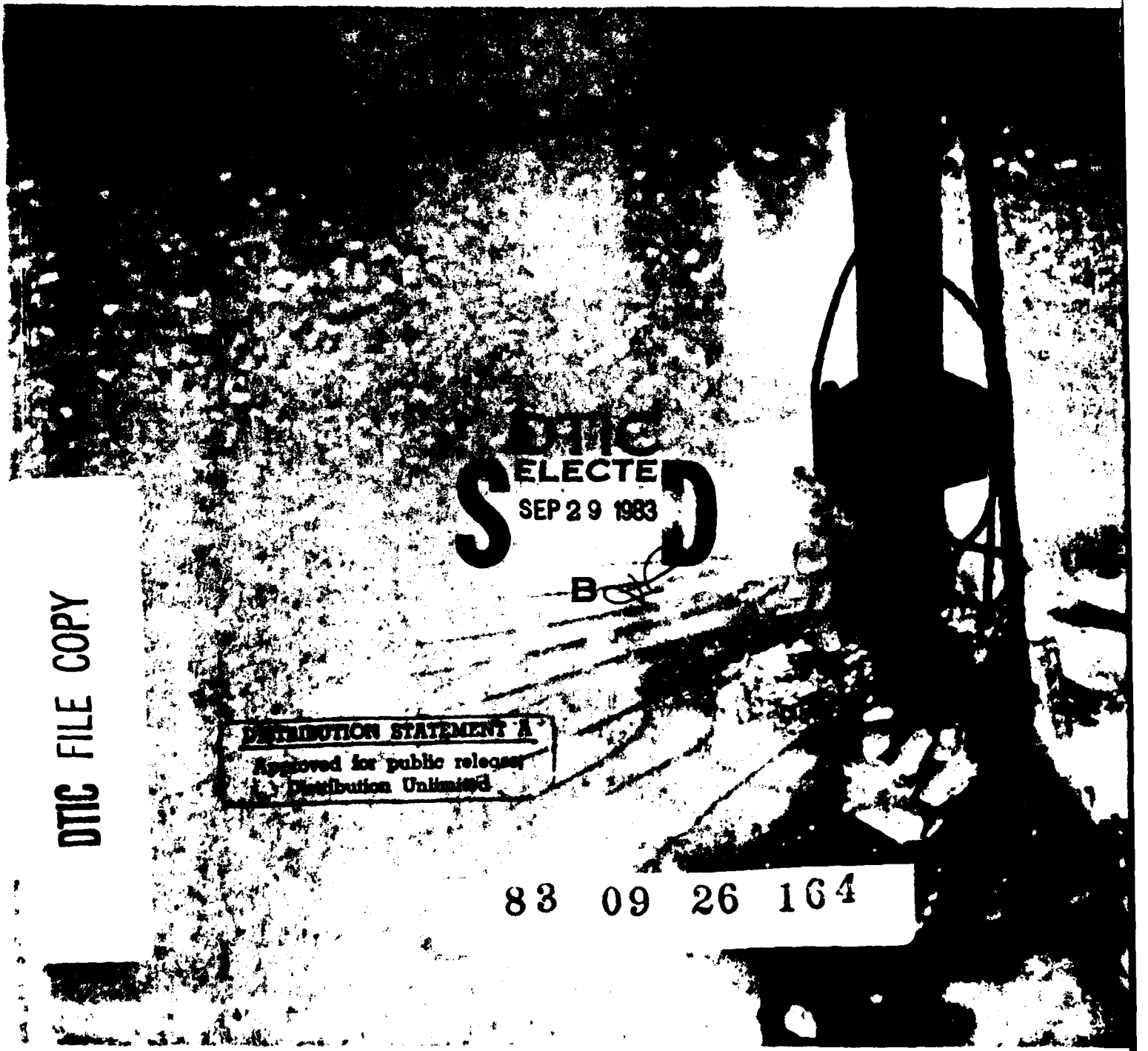

For conversion of SI metric units to U.S./ British customary units of measurement consult ASTM Standard E380, Metric Practice Guide, *published by the American Society for Testing and Materials, 1916 Race St., Philadelphia, Pa. 19103.*

Cover: *A typical flexural failure of an ice sheet showing radial and circumferential cracks.*

CRREL Report 83-19

July 1983

Ice forces on model bridge piers

F.D. Haynes, D.S. Sodhi, K. Kato and K. Hirayama

Prepared for
OFFICE OF THE CHIEF OF ENGINEERS

REPORT DOCUMENTATION PAGE

READ INSTRUCTIONS BEFORE COMPLETING FORM

1. REPORT NUMBER: CRREL Report 83-19
2. GOVT ACCESSION NO.:
3. RECIPIENT'S CATALOG NUMBER:

4. TITLE (and Subtitle): ICE FORCES ON MODEL BRIDGE PIERS
5. TYPE OF REPORT & PERIOD COVERED:
6. PERFORMING ORG. REPORT NUMBER:

7. AUTHOR(s): F.D. Haynes, D.S. Sodhi, K. Kato and K. Hirayama
8. CONTRACT OR GRANT NUMBER(s):

9. PERFORMING ORGANIZATION NAME AND ADDRESS: U.S. Army Cold Regions Research and Engineering Laboratory
Hanover, New Hampshire 03755
10. PROGRAM ELEMENT, PROJECT, TASK AREA & WORK UNIT NUMBERS: CWIS 31723

11. CONTROLLING OFFICE NAME AND ADDRESS: Office of the Chief of Engineers
Washington, D.C. 30214
12. REPORT DATE: July 1983
13. NUMBER OF PAGES: 17

14. MONITORING AGENCY NAME & ADDRESS (if different from Controlling Office):
15. SECURITY CLASS. (of this report): Unclassified
15a. DECLASSIFICATION/DOWNGRADING SCHEDULE:

16. DISTRIBUTION STATEMENT (of this Report): Approved for public release; distribution unlimited.

17. DISTRIBUTION STATEMENT (of the abstract entered in Block 20, if different from Report):

18. SUPPLEMENTARY NOTES:

19. KEY WORDS (Continue on reverse side if necessary and identify by block number)

Bridges	Ice failure
Bridge piers	Ice forces
Cold regions	Model bridge piers
Ice	Model tests

20. ABSTRACT (Continue on reverse side if necessary and identify by block number)
Small-scale laboratory experiments were conducted on model bridge piers in the CRREL test basin. The experiments were performed by pushing model ice sheets against structures and monitoring the ice forces during the ice/structure interaction. The parameters, varied during the test program, were the geometry of the bridge piers and the velocity, thickness, and flexural strength of the ice. The results are presented in the form of ice forces on sloping and vertical structures with different geometries. During ice action on sloping structures, a phenomenon of transition of failure mode from bending to crushing was observed as the ice velocity was steadily increased.

PREFACE

This report was prepared by F.D. Haynes, Research Mechanical Engineer, Dr. D.S. Sodhi, Research Hydraulic Engineer, both of the Ice Engineering Research Branch, Experimental Engineering Division, U.S. Army Cold Regions Research and Engineering Laboratory; K. Kato, Research Engineer, Ishikawajima-Harima Heavy Industries, Tokyo, Japan; and K. Hirayama, Visiting Professor, Iwate University, Japan.

Funding for this research was provided by Corps of Engineers Civil Works Information Project, CWIS 31723, *Model Studies and Ice Effects on Structures*. Dr. J.C. Tatinclaux and D. Cole of CRREL technically reviewed the manuscript of this report.

The contents of this report are not to be used for advertising or promotional purposes. Citation of brand names does not constitute an offical endorsement or approval of the use of such commercial products.

CONTENTS

ILLUSTRATIONS

TABLES

ICE FORCES ON MODEL BRIDGE PIERS

F.D. Haynes, D.S. Sodhi, K. Kato and K. Hirayama

INTRODUCTION

For rational design of structures subjected to ice action, the results of theoretical studies, small-scale laboratory experiments and full-scale measurement of ice forces have to be synthesized to develop guidelines and recommendations in the form of design codes to be used by practicing engineers. Present design codes, such as those of the American Association of State Highway and Transportation Officials (AASHTO 1978) and the Canadian Standards Association (1978), give broad guidelines for estimating the maximum ice force. The recommended effective crushing pressure varies from 700 kPa (100 psi) to 2800 kPa (400 psi), depending upon the condition of the ice at the time of breakup. Besides the guidelines in the design codes, site-specific information is also required on water level variations, and thickness and condition of the ice at the time of breakup.

Ice forces depend mainly on the thickness and properties of the ice, geometry of the structure and the mode of the ice failure or action. Because of high variability of the ice properties, the results of an analytical method to determine ice forces are not likely to be accepted without verifications using full-scale measurement of ice forces. On the other hand, the number of variables influencing the ice forces is so large that the full-scale measured data alone are not useful unless they can be compared to the results of an analytical model. Small-scale experiments play an important role in understanding the action of ice on structures. The results obtained from the laboratory experiments provide information to bridge the gap between theoretical analysis and full-scale measurement by allowing us to assess the influence of various parameters. The object of the present study was to conduct experiments on model bridge piers to determine the effect of velocity, slope angle, shape of piers and aspect ratio (i.e. structure width/ice thickness) on the ice forces on model bridge piers.

TESTS

We conducted the experiments by freezing an ice sheet in CRREL's 33.5-m long, 9.15-m wide and 2.4-m deep refrigerated test basin and pushing it against model structures of different shapes and configurations. The flexural strength and modulus of elasticity of the ice was reduced by dissolving urea (approximately 1% by weight) in water. To grow the ice sheets, air was first bubbled in the water to achieve a uniform temperature of $-0.1\,^{\circ}C$, and the freezing process was started by blowing a mixture of water and air over the water surface in an ambient temperature of $-12\,^{\circ}C$, which resulted in seed ice crystals falling on the water. The resulting ice sheet had three layers as shown in Figure 1: a thin seed layer at the top, a fine-grained transition layer and a coarse-grained bottom layer. The texture throughout was columnar.

Before conducting experiments, we made measurements to determine the thickness, the flexural strength, the characteristic length and the effective modulus of elasticity of the ice sheet. The flexural strength was measured by pushing down on a cantilever beam until it failed. The effective modulus of elasticity was computed from the characteristic length, which was measured by placing dead

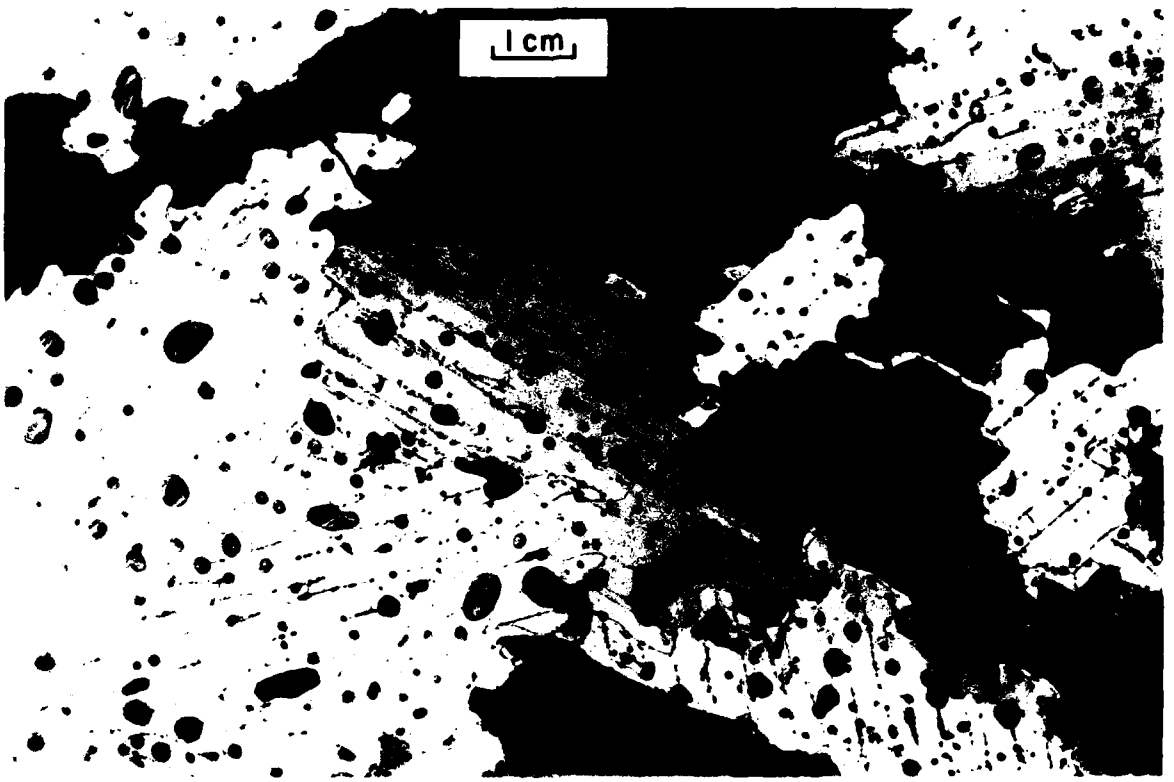

a. Horizontal section in the bottom columnar portion of the ice sheet.

b. Vertical section of the ice sheet.

Figure 1. Thin sections of ice grown in the laboratory from 1% urea solution in water.

weights in discrete increments on a floating ice sheet and monitoring its deformation (Sodhi et al. 1982).

A total of 64 tests were conducted using 22 ice sheets which ranged in thickness from 2.5 to 6.3 cm, in flexural strength from 30 to 257 kPa, in characteristic length from 36 cm to 72 cm and in elastic modulus from 45 to 221 MPa.

We conducted the experiments by pushing an ice sheet against model structures that were attached to a support frame bolted to the bottom of the basin (Fig. 2a). The interchangeable model bridge piers are shown in Figure 2b. Figure 3 shows a test in progress when the ice sheet was pushed against a vertical structure. During each test, the velocity of the ice sheet was increased at a constant rate from 0 to 10 cm/s over a period of 90 seconds. The horizontal force exerted by the ice on the structure was measured by an instrumented support clamp. Although the position of the support clamp could be changed to vary the natural frequency of the system, it was kept at a position to provide maximum stiffness. Accelerometers were attached to the model so that the structural response could be determined in the longitudinal, transverse and torsional modes of vibration.

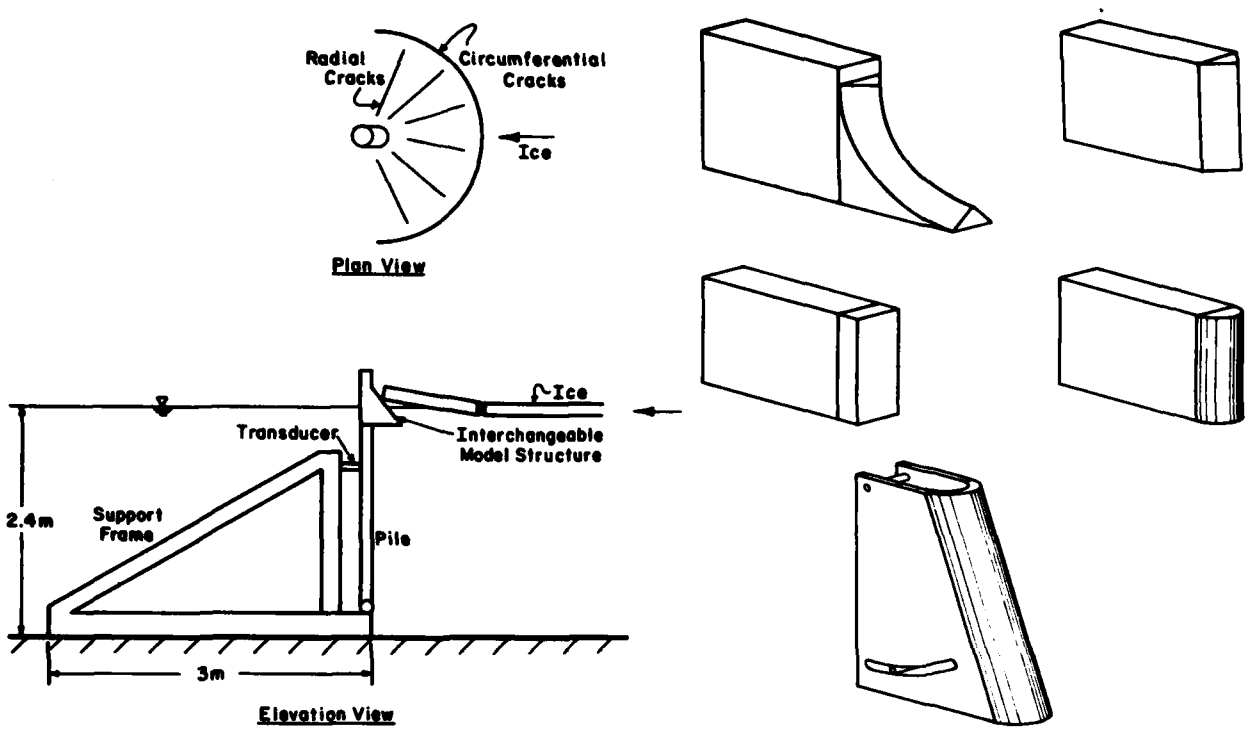

a. Support frame

b. Interchangeable model bridge piers

Figure 2. Test setup.

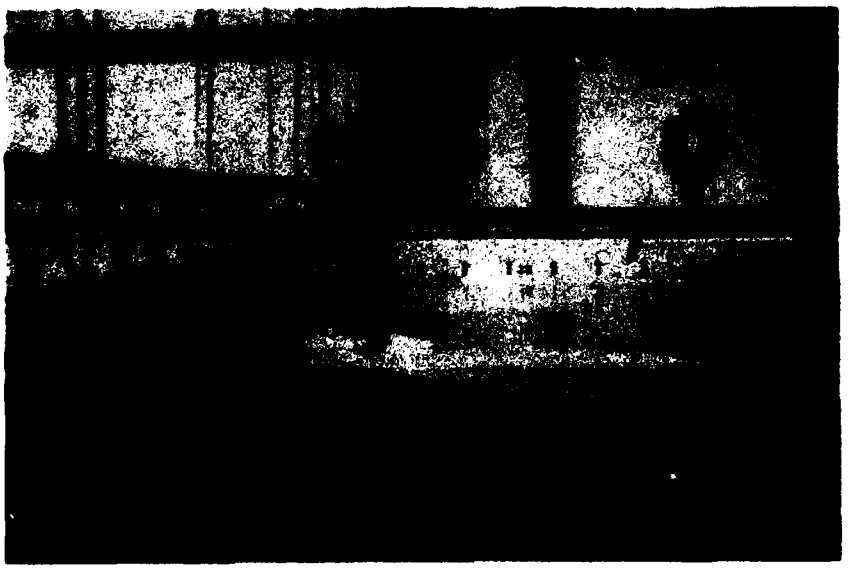

Figure 3. Ice being pushed against a model structure; movement from right to left.

All signals were recorded in analog form on a tape recorder, and the force and velocity signals were also recorded in digital form for data processing. The entire recording system including the data logger was controlled by a computer. Details of the data collection system are given by Määttänen (1979).

RESULTS

The results of this study are presented and discussed in four sections, each concentrating on one aspect of ice-structure interaction: 1) effect of slope angle of inclined structures on the ice forces, 2) change of failure mode from bending to crushing due to increase in ice velocity, 3) effect of aspect ratio on the ice forces, and 4) effect of nose geometry of vertical bridge piers on the forces and vibrations.

Ice forces on inclined structures

A total of 31 tests were conducted on inclined structures (Fig. 4) with slope angles ranging from 52° to 87° from the horizontal. Figure 5 shows radial and circumferential cracks that typically develop when an ice sheet fails by bending as it rides up the inclined structure. We take the first peak in the horizontal ice force record to be the failure load (F) when the velocity of the ice sheet is low. The results of the tests are given in Table 1 where the slope angle, the thickness and the flexural strength of the ice sheet are also listed. During ice action on a sloping structure, both horizontal and vertical forces are generated that are proportional to each other, depending upon the slope angle and the friction angle. The vertical force that bends the ice sheet until it fails is proportional to $\sigma_f h^2$, where σ_f is the flexural strength and h the ice thickness. Field measurements of ice forces on an inclined bridge pier near Hondo, Alberta, by Lipsett and Gerard (1980) also show a dependence

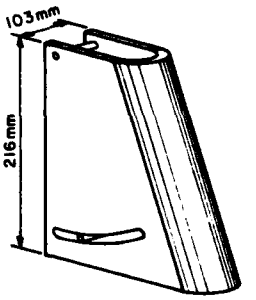

Figure 4. Model inclined bridge pier.

Figure 5. Bending failure of an ice sheet on an inclined structure with a slope angle of 80° from the horizontal. The direction of ice movement is from left to right.

Table 1. Slope angle (α), ice thickness (h), flexural strength (σ_f), ice force (F) and normalized ice force ($F/\sigma_f h^2$) on an inclined structure.

Test number	α *(deg)*	h *(cm)*	σ_f *(kPa)*	F *(kN)*	$F/\sigma_f h^2$
74	52	4.8	77	0.35	1.97
75	69	4.8	77	1.20	6.76
76	52	5.0	78	0.80	4.19
77	69	5.0	78	1.43	7.48
78	87	5.0	78	3.45	18.05
79	87	5.2	77	2.83	13.59
80	56	5.2	77	0.54	2.59
81	73	5.24	77	1.96	9.41
83	80	4.8	128	8.86	30.04
84	73	4.8	128	8.12	27.53
85	66	4.6	96	0.90	4.43
86	59	4.6	96	0.30	1.48
87	52	4.6	96	0.22	1.08
89	69	6.2	100	5.40	14.05
90	66	6.2	100	3.40	8.84
91	87	2.9	63	1.70	32.09
92	80	2.9	63	0.85	16.04
93	73	2.9	63	0.40	7.55
94	80	6.3	31	2.20	17.88
95	59	6.3	31	0.25	2.03
96	52	6.3	31	0.16	1.30
97	52	3.5	45	0.25	4.54
98	59	3.5	45	0.17	3.08
99	66	3.5	45	0.48	8.71
130	65	6.3	87	2.60	7.53
131	67	6.3	87	2.40	6.95
132	70	6.3	87	2.40	6.95
133	73	6.3	87	2.50	7.24
135	68	4.6	70	1.70	11.48
136	75	4.6	70	2.52	17.01
138	80	4.6	70	2.50	16.88

of ice forces on h^2. For that reason and because the tests were conducted with 11 different ice sheets of different thicknesses and flexural strengths, the failure loads have been normalized by $\sigma_f h^2$ and plotted with respect to the slope angle of the structure in Figure 6.

Theoretically, the ratio of the horizontal ice force to the vertical force during an ice action on inclined structures can be shown to be $\tan(\alpha+\phi)$, where α is the slope angle of the structure from the horizontal and ϕ the angle of friction between the structure and the ice. Thus, we expected the normalized ice force ($F/\sigma_f h^2$) to be proportional to $\tan(\alpha+\phi)$ if the vertical force required to bend the ice sheet until failure is constant. The coefficient of

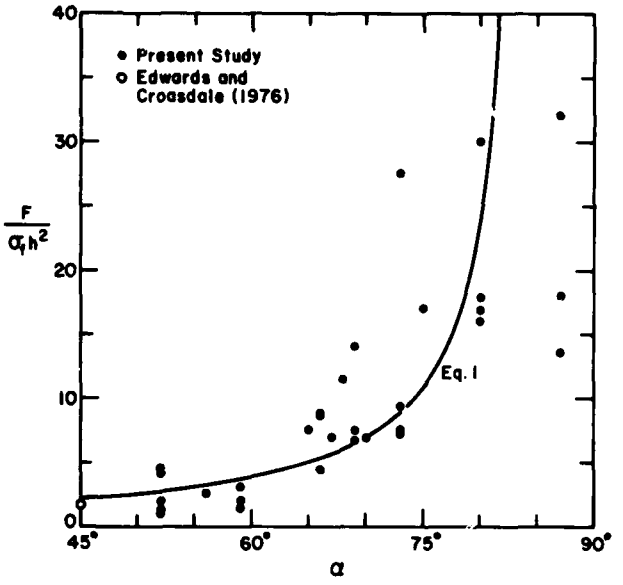

Figure 6. Plot of normalized ice force ($F/\sigma_f h^2$) on an inclined structure with respect to the slope angle α. For these tests the coefficient of friction was 0.1 and the width of structure was 10.3 cm.

friction μ ($=\tan\phi$) was measured through friction tests (Haynes et al. 1982), and its average value was determined to be 0.1 for steel and ice. Thus, the angle of friction ϕ was 5.7°. A curve of best fit was found between the data points of ($F/\sigma_f h^2$) and $\tan(\alpha+5.7°)$ by nonlinear regression in which the data points at $\alpha = 87°$ were not taken into consideration for computational reasons. The equation of the best fit curve is given as

$$F/\sigma_f h^2 = 1.78\tan(\alpha+5.7°). \quad (1)$$

A plot of the above equation is also shown in Figure 6. The scatter in the data is large for high values of α compared to that for small values of α. We saw that some of the failures at high values of α were caused by a combination of buckling and bending.

Edwards and Croasdale (1976) conducted experiments on 45° angle cones. The ice breaking component of the force from their study is plotted in Figure 6 at $\alpha = 45°$, and there is good agreement between their test results and eq 1.

Frederking (1980) conducted tests on a 45° inclined plane and analyzed ice forces due to bending failure of the ice sheet, hydrodynamic drag between the water and the ice, inertial effects of broken pieces of ice, friction between the ice and the structure, and gravity.

The experimental results in Table 1 are compared with the plastic limit analysis by Ralston (1977) of the breaking component of the ice force; this comparison is shown in Figure 7 for values of $\alpha < 85°$ and $\mu = 0.1$. Since Ralston's analysis was for a conical structure and our tests were conducted on a sloping cylindrical structure, a strict comparison cannot be made. In spite of this, there is some agreement between the present force data and the forces predicted by Ralston's formulation. Overall, however, our experimental results tend to be higher than the theoretical ice forces from Ralston's formulation.

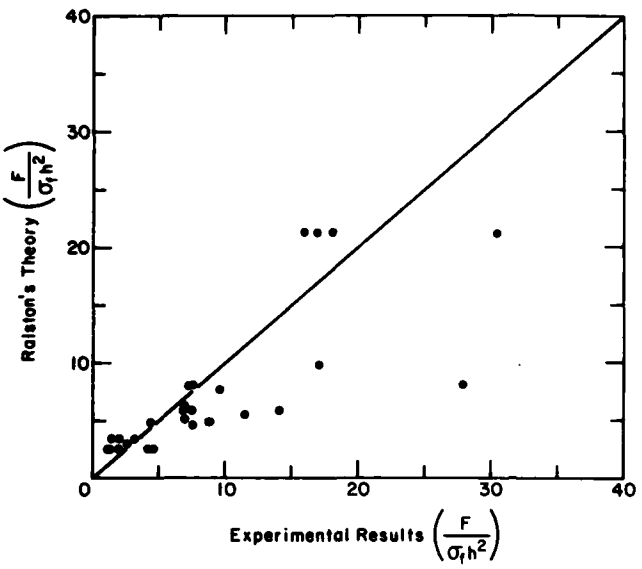

Figure 7. Comparison of experimental results with those predicted by Ralston's (1977) formulation.

Transition of ice action due to velocity increase

As mentioned earlier, we increased the velocity of the ice sheet at a constant rate from 0 to 10 cm/s over a period of 90 seconds during each test. During the tests with inclined structures, we observed a transition in the failure mode at a certain velocity (hereafter called transition velocity) from predominantly bending to predominantly crushing. Figure 8 is a photograph of the successive circumferential cracks that were formed during the bending failure of the ice sheet. Figure 9 shows the failure mode changing from large circumferential cracks to a narrow path with crushed ice on each side of it.

After extensive field measurement of ice forces, Neill (1976) and Lipsett and Gerard (1980) reported both bending and crushing failure of an ice sheet against an inclined bridge pier (23° from the vertical) in the Athabasca River near Hondo, Alberta. This observation has implications when we consider design forces for a sloping bridge pier because the possibility of crushing along with bending failure exists at high ice velocity.

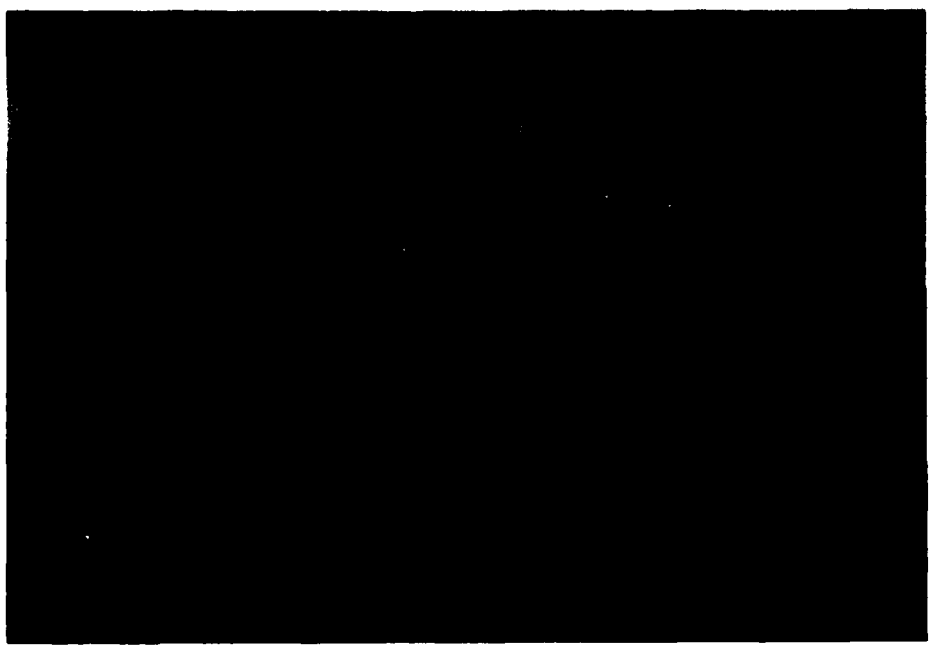

Figure 8. Track of the model structure showing bending failure of the ice in successive circumferential cracks.

Figure 9. Transition in failure mode from bending (circumferential cracks) to crushing (rubble pile on both sides of track).

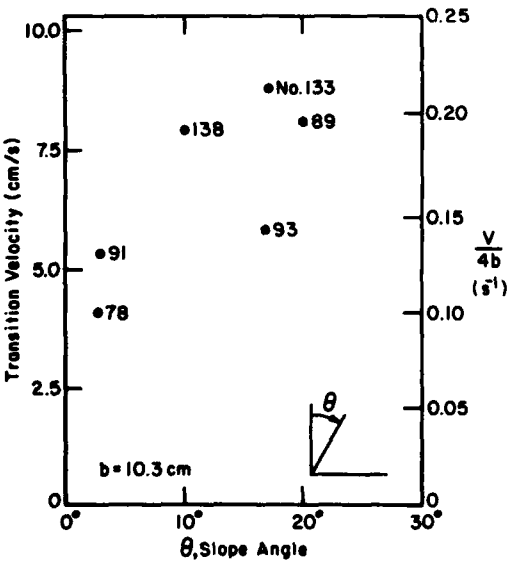

Figure 10. Transition velocity with respect to slope angle. The numbers beside the data points refer to the test number, for which the ice properties and thickness are given in Table 1. The scale on the right ordinate indicates an empirical strain rate proposed by Michel and Toussaint (1976).

As mentioned earlier, the ice action on an inclined structure results in both horizontal and vertical forces. When the velocity of an ice sheet is low, the vertical force is mainly caused by the weight and elastic forces from a portion of the ice sheet near the contact area. As the velocity of the ice sheet increases, the kinematics of the ice-structure interaction requires high acceleration of the ice sheet and water in the vertical direction during lifting. This acceleration results in an increase in the vertical forces at the ice-structure contact area. When the force required to lift the ice sheet exceeds the force required to cause the ice sheet failure in shear or in crushing, a transition in the failure mode takes place.

The results of our experiments are shown in Figure 10, in which transition velocity is plotted with respect to the angle from the vertical of the inclined structure. A trend of higher transition velocity with increased angle from the vertical can be seen in Figure 10. The trend seems reasonable because the crushing failure is likely to take place at a lower transition velocity for almost vertical structures.

Aspect ratio

Previous experimental and analytical work has identified the effect of aspect ratio (structure width/ice thickness) on ice crushing force against

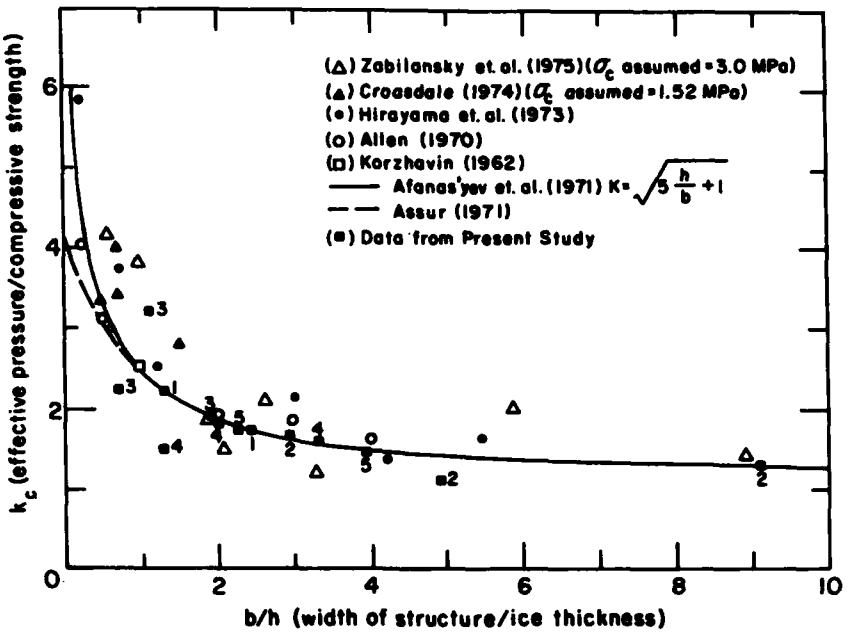

Figure 11. Aspect ratio effect on effective pressure during crushing failure of ice (after Neill [1976] and Lipsett and Gerard [1980]). The numbers beside the data points refer to the ice sheet number used in this study

vertical structures. This effect is an increase in effective ice pressure as the width of the structure becomes small in relation to the ice thickness. For the present study, the range of aspect ratio was from 0.7 to 9.0. Results are shown in Figure 11 along with the results of other studies for comparison.

To compare the results of different tests conducted on a given ice sheet, the compressive strength was estimated from the ice force data of the test with the maximum aspect ratio and the ice force equation proposed by Afanas'yev et al. (1971). The above procedure was adopted because there is no satisfactory technique developed to measure the in situ compressive strength of model ice. In Figure 11 the ratio of the normalized effective pressure to compressive strength is plotted with respect to aspect ratio, and the numbers beside the data points refer to the ice sheet number used in this study. The results of the present study show the effect of aspect ratio on the effective pressure during crushing failure of the ice sheet, and the scatter in the data is about the same as that from the other studies shown in Figure 11.

Bridge pier nose geometry

The objective of this series of tests was to compare ice forces and vibration levels during ice action against vertical bridge piers with different nose geometries (Fig. 12) and a curved bridge pier (Fig. 13). A set of tests consisted of four tests with one ice sheet using the interchangeable model bridge piers shown in Figures 12 and 13. Besides measuring the ice forces with the help of an instrumented clamp, we placed three accelerometers on the model bridge pier to determine accelerations in the longitudinal, transverse and torsional modes of vibration.

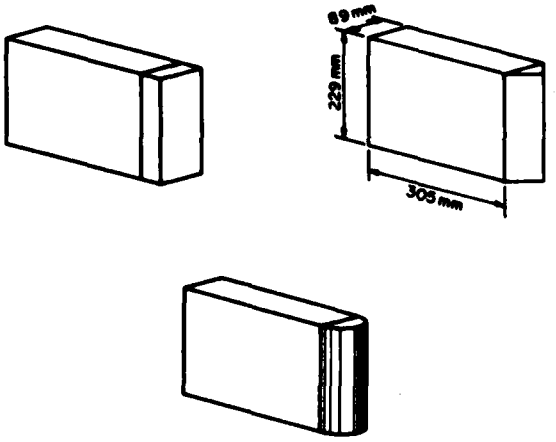

Figure 12. Model vertical bridge piers with different nose geometries.

The results of the five test series are presented in Table 2 in which the averages of the five highest force levels are listed. The thickness and flexural strength of the ice sheets used in the five test series are also listed in Table 2. The averages of the maximum ice force are also shown graphically in Figure 14 for comparison.

It can be seen in Figure 14 that the curved bridge pier (Fig. 13) induces the least ice force due to flexural failure. Most bridge piers are either sloped or curved to cause ice failure by bending. However, the curved pier's use may be limited because it is only effective in reducing the ice forces as long as the ice impinges on the sloping part of the pier. During spring breakup of river ice, there is usually a large, rapid rise in water level that effectively breaks and transports the ice. In such situations the vertical bridge piers are generally designed to resist the ice action (e.g., the bridge piers in the Yukon River). Comparing the ice force levels in Figure 14, we see no clear advantage in adopting a particular geometrical shape for the vertical bridge pier nose because the force levels are of the same order of magnitude. The ice forces show an overall increase with increasing flexural strength, which usually increases with increasing compressive strength. The ice force on the round nose was less in three out of five comparisons, but it was higher when the flexural strength of the ice was high. However, the data from the present study do not permit us to make a general conclusion based on the ice force levels alone.

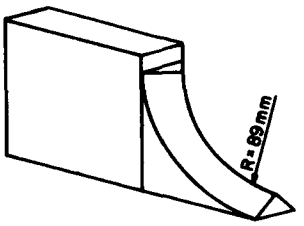

Figure 13. Model curved bridge pier.

The acceleration of the bridge pier was monitored for longitudinal, transverse and torsional modes of vibration. The vibration levels of the bridge piers were compared to the flat-nose bridge

Table 2. Ice force data for different bridge pier geometries (the width of bridge pier was 8.9 cm [3.5 in.]).

Test number	*Ice thickness (cm)*	*Flexural strength (kPa)*	*Pier nose geometry*	*Average of 5 highest force levels (N)*	*Standard deviation of 5 highest force levels (N)*	*Ratio of standard deviation to average force (%)*
101	3.0	49	Round	1120	76	7
102	3.0	49	Pointed	1980	306	15
103	3.0	49	Flat	2640	421	16
104	3.0	49	Curved	190	0	0
110	4.6	69	Pointed	4220	340	8
111	4.6	69	Round	4270	591	14
112	4.6	69	Curved	2780	81	3
113	4.6	69	Flat	3940	162	4
114	2.7	257	Flat	4910	491	10
115	2.7	257	Round	6560	720	11
116	2.7	257	Pointed	5910	254	4
117	2.7	257	Curved	2110	98	5
120	3.8	96	Flat	3360	95	3
121	3.8	96	Round	3130	135	4
122	3.8	96	Pointed	4050	102	3
123	3.8	96	Curved	540	34	6
124	2.7	48	Curved	90	34	40
126	2.7	48	Round	2450	128	5
127	2.7	48	Pointed	2500	52	2
128	2.7	48	Flat	2910	838	29

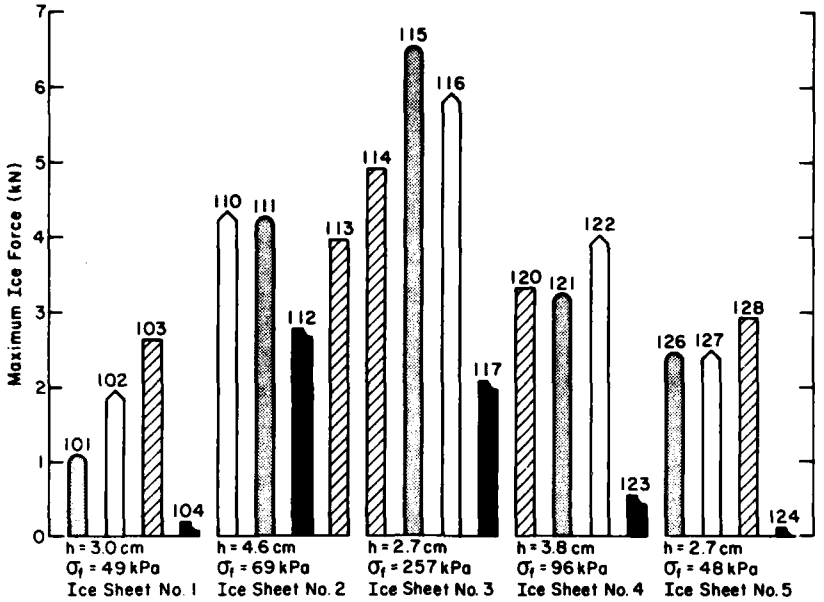

Figure 14. Comparison of ice forces for different configurations and nose geometries of the bridge piers (numbers correspond to test numbers in Table 2; shape of histogram indicates nose geometry).

pier. The relative acceleration levels in the longitudinal direction were 77, 90 and 24% for the round, pointed and curved bridge piers respectively. The similar figures for the transverse directions were 80, 99 and 73% for the round, pointed and curved bridge piers respectively. Data for the torsional vibration are yet to be analyzed and will be presented in a later report. The curved bridge piers induced the lowest acceleration levels from flexural failure of the ice sheet. Of the three shapes of the vertical bridge pier, the round-shaped nose induced the lowest acceleration levels, and this may be attributed to the uniformity of the contact between the round-shaped pier and the ice sheet. The pointed nose sometimes engages the ice unsymmetrically on one side, which induces considerable torsional acceleration as the pier nose intrudes into the ice sheet in a slightly zigzag path. This was also observed for a pointed-nose bridge pier in the Yukon River by McFadden et al. (1981).

CONCLUSIONS

On the basis of the experimental results, we make the following conclusions:

1. The ice force required to bend an ice sheet until failure is strongly influenced by the slope angle of the inclined structure; this trend is in accordance with theory.

2. As the velocity of the ice sheet moving against an inclined structure was increased at a constant rate, the mode of failure changed from bending to crushing at a certain velocity. This transition velocity increases with the slope angle from the vertical. We attribute the change failure mode to the development of inertia forces during lifting up of the ice sheet.

3. The experimental data of this study support the previously identified aspect ratio effect during the crushing failure of ice against vertical structures. Because there is still no satisfactory method for measuring in situ compressive strength of ice, we could not conduct a systematic study of the effect of different aspect ratios and different coefficients of friction between ice and structure.

4. The comparative testing of ice action on different geometries of bridge piers indicated that the curved pier induced the lowest levels of ice forces and accelerations. The vertical bridge piers induced similar ice forces vibrations. However, the round-shaped nose of the vertical bridge piers had the lowest level of ice forces and vibrations.

Additional work needs to be done in the laboratory and in the field to measure ice forces from the crushing failure of ice at different velocities. The influence of coefficent of friction between the ice and structures needs further investigation as well.

LITERATURE CITED

Afanas'yev, V.P., I.V. Dolgopolov and Z.I. Shvayshtein (1971) Ice pressure on separate supporting structures in the sea. USA Cold Regions Research and Engineering Laboratory, Draft Translation 346. AD 741873.

Allen, J.L. (1970) Effective force of floating ice on structures. National Research Council of Canada Technical Memorandum 98. Ottawa.

American Association of State Highway and Transportation Officials (1978) Interim specifications for Highway Bridges. Washington, D.C., pp. 27–28.

Assur, A. (1971) Forces in moving ice-fields. *Proceedings, First International Conference on Port and Ocean Engineering under Arctic Conditions, August 23–30, Trondheim, Norway.* Technical University of Norway, pp. 112–118.

Canadian Standards Association (1978) Design of Highway Bridges. Standard CAN3-56-M78. Ottawa, pp. 34–36.

Croasdale, K.R. (1974) The crushing strength of arctic ice. *Proceedings, Symposium on Beaufort Sea Coastal and Shelf Research.* Montreal, Quebec: Arctic Institute of North America.

Edwards, R.Y. and K.R. Croasdale (1976) Model experiments to determine ice forces on conical structures. *Journal of Glaciology,* 19(81): 660.

Frederking, R. (1980) Dynamic ice forces on an inclined structure. In *Physics and Mechanics of Ice.* New York: Springer-Verlag, pp. 104–106.

Haynes, F.D., K. Hirayama, K. Kato and D.S. Sodhi (1982) Friction tests on model ice. USA Cold Regions Research and Engineering Laboratory, Internal Report 744.

Hirayama, K., J. Schwarz and H. Wu (1973) Model technique for the investigation of ice forces on structures. *Proceedings, Second International Conference on Port and Ocean Engineering under Arctic Conditions, August 27–30, Reykyavik, Iceland.* University of Iceland, pp. 332–344.

Korzhavin, K.N. (1962) Action of ice on engineering structures. USA Cold Regions Research and Engineering Laboratory, Draft Translation 260. AD 723169.

Lippsett, A.W. and R. Gerard (1980) Field measurements of ice forces on bridge piers,1973–1979. Alberta Research Council Report No. SWE 80-3. Edmonton, Alberta.

Määttänen, M. (1979) Laboratory tests for dynamic ice-structure interaction. *Proceedings, Fifth International Conference on Port and Ocean Engineering under Arctic Conditions (POAC 79), August 13–18, Trondheim, Norway.* Norwegian Institute of Technology, pp. 1139–1153.

McFadden, T., F.D. Haynes, J. Burdick and J. Zarling (1981) Ice force measurement on the Yukon River bridge. *ASCE Specialty Conference, April, Seattle, Washington.* New York: American Society of Civil Engineers, pp. 749–777.

Michel, B. and N. Toussaint (1977) Mechanisms and theory of indentation of ice plates. *Journal of Glaciology,* 19(18): 285–300.

Neill, C.R. (1976) Dynamic ice force on piers and piles: An assessment of design guidelines in the light of recent research. *Canadian Journal of Civil Engineering,* 3(2): 305–341.

Ralston, T.D. (1977) Ice force design consideration for conical offshore structures. *Proceedings, Fourth International Conference on Port and Ocean Engineering under Arctic Conditions, September 26–30, St. Johns, Newfoundland.* Memorial University of Newfoundland, pp. 741–751.

Sodhi, D.S., K. Kato, F.D. Haynes and K. Hirayama (1982) Determining the characteristic length of model ice sheets. *Cold Regions Science and Technology:* 6(2): 99–104.

Zabilansky, L.J., D.E. Nevel and F.D. Haynes (1975) Ice forces on model structures. *Canadian Journal of Civil Engineering,* 2(4): 400–407.

A facsimile catalog card in Library of Congress MARC format is reproduced below.

Haynes, F.D.
Ice forces on model bridge piers / by F.D. Haynes, D.S. Sodhi, K. Kato and K. Hirayama. Hanover, N.H.: U.S. Cold Regions Research and Engineering Laboratory; Springfield, Va.: available from National Technical Information Service, 1983.
iii, 17 p., i/lus., 28 cm. (CRREL Report 83-19.)
Prepared for the Office of the Chief of Engineers by Corps of Engineers, U.S. Army Cold Regions Research and Engineering Laboratory.
Bibliography: p. 11.
1. Bridges. 2. Bridge piers. 3. Cold regions. 4. Ice. 5. Ice failure. 6. Ice forces. 7. Model bridge piers. 8. Model tests.

(see next card)

Haynes, F.D.
Ice forces on model bridge piers (Card 2)

I. Sodhi, D.S. II. Kato, K. III. Hirayama, K.
IV. United States. Army. Corps of Engineers.
V. Cold Regions Research and Engineering Laboratory, Hanover, N.H. VI. Series: CRREL Report 83-19.


FIL